

ATMOSPHERIC DYNAMICS AND SHOCK WAVES IN THE PULSATING STAR RR Lyr

Mauclaire, B.¹, Mathias, Ph.² and the GRRR Collaboration³

Abstract. During the annual Spectro star party organized at the OHP in 2012, Denis GILLET presented the study of shock waves in pulsating stars. Intriguing aspects were the modulation of the luminosity maxima by the Blazhko effect and the development of a physical model describing atmospheric dynamics. A pro-am collaboration* which still goes on was born resulting in the publication of 2 articles in A&A.

Keywords: shock waves, stars: variables: RR Lyrae, stars: individual: RR Lyr, stars: atmospheres, professional-amateur collaboration

1 Introduction

RR Lyrae stars are population II pulsating stars located at the bottom of the Instability strip. They show large amplitude motion, driven by strong shock waves, the propagation of which producing remarkable observational facts such as line doubling and blueshifted emission. Some of these stars, including the prototype, present a long-term modulation of light maxima called the Blazhko effect.

Preston et al. (1965) reported the first detailed spectroscopic study of RR Lyr during a whole Blazhko cycle, but this investigation was limited to the rising part of the light curve. Using new spectroscopic observations, Preston (2011) and Chadid & Preston (2013) studied atmosphere dynamics of various RR Lyrae stars, except RR Lyr itself. In particular, they sometimes detected a weak and redshifted emission within the H α profile, occurring around the pulsation phase $\varphi = 0.30$, that they called the third apparition. In order to investigate this phenomenon in RR Lyr and more widely the atmosphere dynamics, a pro-am collaboration started in 2013 performed a high time rate spectroscopic campaign.

2 Observations and data analysis

To monitor the different phenomena occurring within the atmosphere, high time rate (5 to 15 min) data were collected from different instruments:

- ELODIE spectrograph: Attached to the 193 cm telescope at the Observatoire de Haute-Provence, its resolving power is $R = 44,000$ (Baranne et al. 1996). In the context of a survey (1994 – 1997) led by D. Gillet and published in Chadid et al. (1999), we selected 6 spectra, having an S/N between 63 and 91.
- AURELIE spectrograph: 28 spectra were obtained in 2013 – 2014 aimed to detect the third apparition in the H α line. This spectrograph, attached to the 152 cm telescope at the Observatoire de Haute-Provence (Gillet et al. 1994), allowed us to obtain spectra having $R = 22,700$ and a mean S/N of 85.
- ESHELL spectrograph: Attached to an automated 35 cm telescope at the Observatoire de Chelles (France), this fiber-fed eShel spectrograph described in Thizy & Cocharad (2011), allowed us to collect 85 spectra during April 2017 with $R = 10,500$ and a mean S/N of 74.

¹ Observatoire du Val de l'Arc, 13530 Trets, France

² IRAP, Université de Toulouse, CNRS, UPS, CNES, 57 avenue d'Azereix, 65000, Tarbes, France

³ Observatoire de Haute-Provence, 04870 Saint-Michel l'Observatoire, France

* The *Groupe de Recherche sur RR Lyrae* (GRRR) is an association of professionals and amateur astronomers leading high-resolution spectroscopic and photometric monitoring of complex phenomena such as the RR Lyrae Blazhko effect.

Spectra were homogeneously processed with pipelines that perform classical operations. In particular, all spectra are delivered in the stellar rest frame in order to easily study the atmosphere dynamics. All wavelengths (λ) are given in \AA (Angström). Analysis was performed with SpcAudace software (Mauclaire 2017).

3 First observation of $H\alpha$ redshifted emission in RR Lyr

3.1 Datasets

Between 2013 and 2015, the third apparition has been observed five times. Because this spectral feature consists in a weak hump and since exposures are short (600 s), we selected observations with the best S/N: 2014-09-14 and 2013-09-04 nights. Figure 1 presents spectral time series around $\varphi = 0.3$ where the third emission is rising (left panel) or fading (central panel).

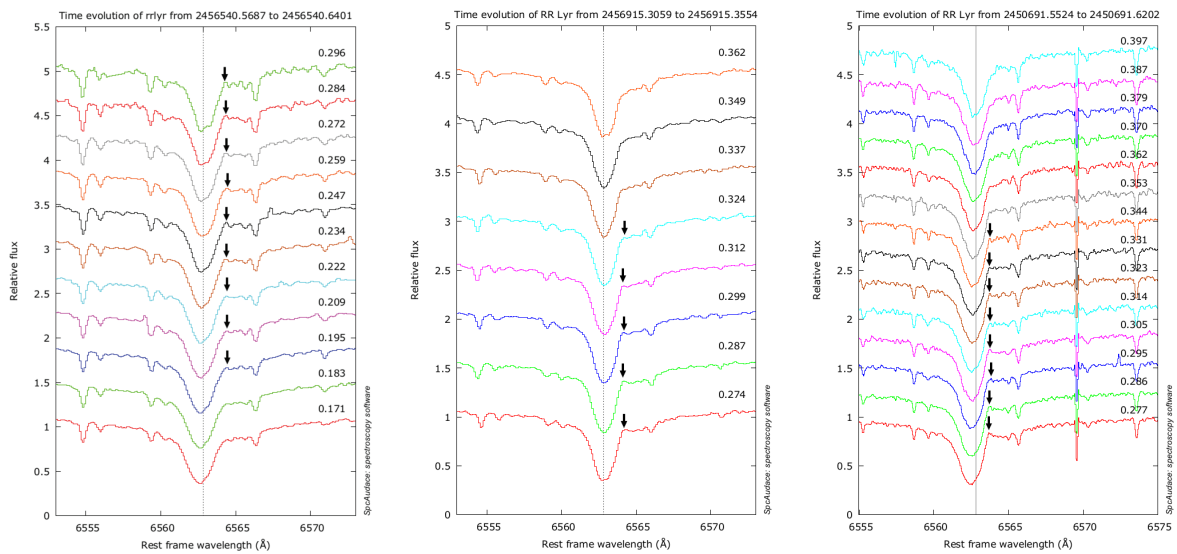


Fig. 1. The third apparition at 3 different dates represented in the stellar rest frame. The vertical line indicates the $H\alpha$ line laboratory wavelength. Weak absorptions are telluric lines. The small hump on the red edge of the $H\alpha$ line is the third apparition, highlighted with black arrows. **Left panel:** AURELIE 2013-09-04 time series. **Central panel:** AURELIE 2014-09-14 time series. **Right panel:** ELODIE 1997-08-30 archive.

Observations show that the third emission is present in every pulsation cycle near $\varphi = 0.3$ i.e., just after the maximum light amplitude. As it is observed at different Blazhko phases, this phenomenon might be independent of the Blazhko effect.

3.2 Physical origin of the hydrogen third emission

The pulsation engine induces the main shock that appears in the stellar atmosphere around phase $\varphi \sim 0.92$. Its immediate effect is to rise the different layers crossed along its outward propagation. Around phase $\varphi \sim 0.3$, the deepest photospheric layers are close to their maximum radius (Fokin & Gillet 1997). Their velocity is therefore close to zero before they will start their fall back onto the star. However, the main shock coming with the actual pulsation cycle still propagates outward, encountering the upper atmosphere located at approximately 1.35 photospheric radius. In addition, its intensity has decreased since it is not able to produce a blueshifted emission component within the $H\alpha$ profile: the shock is thus no longer radiative.

Ahead of this shock front, the layers have not yet completed their infalling motion induced by the previous pulsation cycle. The infalling motion of these highest atmospheric layers compresses the gas located in front of the shock that, by its outward motion, contributes to this large compression. It thus can be inferred that the third $H\alpha$ apparition is produced within this strongly compressed zone, hence high-temperature zone, that exists immediately above the shock front.

4 Dynamical structure of the atmosphere

4.1 Observation strategy

The pro-am collaboration led to a further study of the atmosphere dynamics, focusing now along the entire pulsation cycle. However, since the RR Lyr pulsation period is 13.6 h, it is not easy to cover a whole cycle within a single night. Moreover, in addition to the Blazhko effect, differences between non consecutive pulsation cycles issued from the non-linear character of the atmosphere dynamics may blur the visibility of the different involved phenomena. Therefore, it is necessary to observe the star as often as possible, taking advantage of each good weather conditions.

This constraining situation led us to build an automated high resolution spectroscopic setup based on a T35 cm at the Observatoire de Chelles (Lemoult et al. in prep.). Based on an echelle spectrograph, the spectral range spans from 4 300 to 7 100 Å for a resolving power of $R = 10,500$ at $\lambda 5896.92$. This setup allowed more than 47 h of observations within only 11 d, with a 15 min time resolution. These 11 d represent 28% of a Blazhko cycle, allowing to focus on the different phenomena that occur during a typical pulsation cycle. Hence, a detailed study of the atmosphere dynamics of RR Lyr during consecutive pulsation cycles was possible for the first time.

4.2 Atmospheric dynamics scenario

Figure 2 displays some spectra obtained during the campaign for two lines: $H\alpha$ and Na D1. Both lines present a line doubling phenomenon, but because the red component of the Na D1 line has a constant velocity, its presence is attributed to the interstellar medium (ISM). The $H\alpha$ blue emission associated to the main shock is easily detected around $\varphi \sim 0.9$ i.e., immediately before the line doubling phenomenon, while the one corresponding to the second apparition ($\varphi \sim 0.7$) is rather weak.

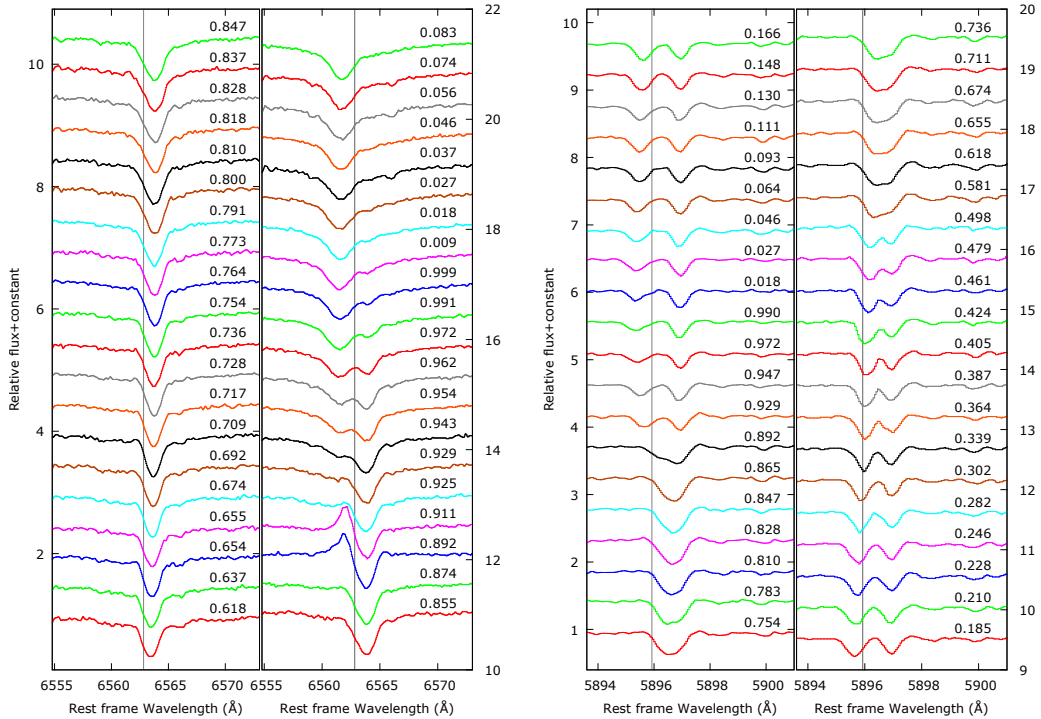


Fig. 2. Part of April 2017 time series represented in the stellar rest frame at different pulsation phases. The vertical line is the laboratory wavelength of the studied line. The time resolution is 15 min. **Left panel:** $H\alpha$ line with first apparition near $\varphi \sim 0.91$ followed by a line doubling. **Right panel:** Na D1 line, where the red component originates from the ISM.

From the evolution of the different observed phenomena such as line doubling, blue- or red-shifted emissions (in particular the 3 apparitions within the $H\alpha$ profile), $H\alpha$ layer lagging behind that of Na (Fig. 3), we determined the main dynamic phenomena occurring in the atmosphere of RR Lyr during a pulsation cycle:

- $\varphi = 0.874 - 0.892$: emergence of the main shock, originating in the subphotospheric layers (κ -mechanism);
- $\varphi = 0.892 - 0.929$: radiative shock wave phase *i.e.*, the $H\alpha$ line presents a well-marked blue-shifted emission, the first apparition. The doubling phenomenon shows the reversal motion from ballistic infall into rising due to the outward shock wave propagation. The main shock is however decelerating;
- $\varphi = 0.320$: maximum expansion of the Na layer, rather formed in the lower atmosphere;
- $\varphi = 0.455$: maximum expansion of the $H\alpha$ layer *i.e.*, the main shock propagates now in the upper layers;
- $\varphi = 0.320 - 0.455$: two-steps infalling motion, the region just ahead of the shock is strongly compressed between the main shock and the ballistic motion of the upper layers. Observation of the small redshifted $H\alpha$ emission corresponds to the third apparition;
- $\varphi = 0.600 - 0.874$: the upper layers end their ballistic motion onto the deeper layers, producing a small blueshifted emission *i.e.*, the second apparition. Note that the intensity of this emission is directly Blazhko phase dependent.

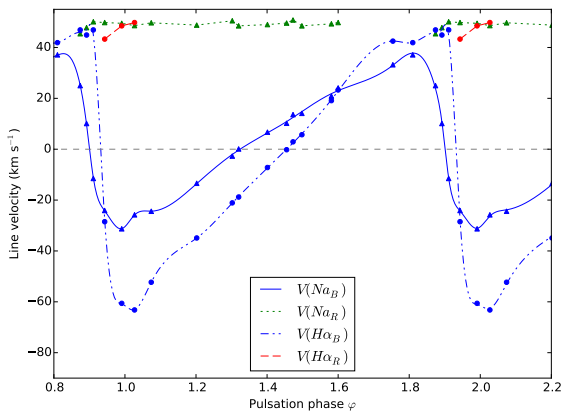


Fig. 3. Curves of velocity with respect to the stellar rest frame of the sodium and $H\alpha$ over the pulsation phase $\varphi = 0.8$ to $\varphi = 2.2$. Shown are the blue components, $V(Na_B)$ (blue filled line) and $V(H\alpha_B)$ (blue dot-dashed line), and their respective red components, $V(Na_R)$ (green dotted line) and $V(H\alpha_R)$ (red dashed line). The mean uncertainty is $\pm 0.6 \text{ km s}^{-1}$.

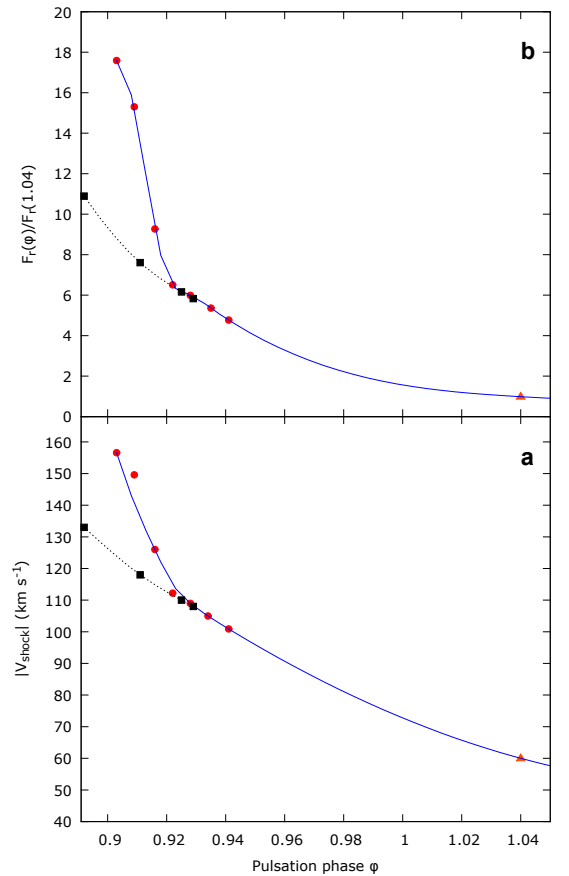


Fig. 4. Panel a: Phased evolution of $|V_{\text{shock}}|$ plotted with a trend curve. Thus, for 40% of the period, the shock front velocity decreases by a factor of more than three. **Panel b:** Evolution of maximum values of radiative flux $F_r(\varphi)/F_r(1.04)$ ratio plotted with a trend curve. The flow of radiative losses increases rapidly with the speed of the shock front.

In addition to these phenomena, it was also possible to monitor the energy of the main shock plotted in Fig. 4. Whereas Preston et al. (1965) showed that during its outward propagation, the shock increases in

intensity and velocity, our observations only show the shock deceleration. Indeed, during the first apparition ($\varphi = 0.90 - 1.04$), the shock front velocity decreases from 155 km s^{-1} (leading to a Mach number $M \sim 15$) down to 60 km s^{-1} as shown in Fig. 4, involving 2 mechanisms:

- (strong) radiative losses until $\varphi \sim 0.95$;
- dilution phenomena in the second part.

It is also shown that this energy modulation may be strongly influenced by the Blazhko phase.

5 Conclusion

The first part of the pro-am collaboration demonstrates the presence of this third apparition in RR Lyr itself, where it is clearly detected in the phase interval $\varphi = 0.188 - 0.407$ i.e., during about 20% of the pulsation period. With a peak representing 13% of the continuum, the emission intensity is very weak, and appears on the red side of the $H\alpha$ line profile. This work led to a refereed publication: Gillet et al. (2017). In particular, this article was the first one where an amateur actively contributed to both data analysis and redaction.

The second part of this collaboration concerned the atmospheric dynamics of RR Lyr along a typical pulsation cycle. One of the main result is the shock wave energy modulation, with first an isothermal shock cooled from radiative losses, followed by an adiabatic cooling through wave front density dilution. These results are described in a second refereed publication (Gillet et al. 2019).

This still ongoing, fruitful, collaboration, gathering more than 20 “amateurs”, points out the importance of a still low used observation method: medium spectroscopic resolution ($R \sim 10,000$, but it is however sufficient for most of this kind of studies, even applied to other stars) combined to high time rate allows important physical process refinements. As a consequence, such pro-am collaborations should be encouraged.

References

- Baranne, A., Queloz, D., Mayor, & al. 1996, A&AS, 119, 373
 Chadid, M., Kolenberg, K., Aerts, C., & Gillet, D. 1999, A&A, 352, 201
 Chadid, M. & Preston, G. W. 2013, MNRAS, 434, 552
 Fokin, A. B. & Gillet, D. 1997, A&A, 325, 1013
 Gillet, D., Burnage, R., Kohler, D., & al. 1994, A&AS, 108, 181
 Gillet, D., Mauclore, B., Garrel, T., & al. 2017, A&A, 607, A51
 Gillet, D., Mauclore, B., Lemoult, T., et al. 2019, A&A, 623, A109
 Mauclore, B. 2017, SpcAudace: Spectroscopic processing and analysis package of Audela software, Astrophysics Source Code Library
 Preston, G. W. 2011, AJ, 141, 6
 Preston, G. W., Smak, J., & Paczynski, B. 1965, ApJS, 12, 99
 Thizy, O. & Cochard, F. 2011, in IAU Symposium, Vol. 272, Active OB Stars: Structure, Evolution, Mass Loss, and Critical Limits, ed. C. Neiner, , G. Wade, , G. Meynet, & G. Peters, 282–283

Total (abstract+project presentation) characters count leads to 14820 and was performed with following commands:
`pdftotext file.pdf ; wc -m file.txt.`